Proceedings of ESSCIRC, Grenoble, France, 2005

Ultra Low-power Analog Morlet Wavelet Filter in 0.18 μm BiCMOS Technology

Sandro A. P. Haddad [1], Joel M. H. Karel [2], Ralf L. M. Peeters [2],
Ronald L. Westra [2] and Wouter A. Serdijn [1]
(1) Delft University of Technology, Mekelweg 4, 2628 CD Delft, The Netherlands .
(2) University of Maastricht P.O.Box 616, 6200 MD, Maastricht, The Netherlands.
[s.haddad, w.a.serdijn]@ewi.tudelft.nl,
[joel.karel,ralf.peeters,westra]@math.unimaas.nl

Abstract:

A novel procedure to implement the wavelet transform using analog circuitry is presented. First, an approximation is used to calculate the transfer function of the filter, whose impulse response is the required wavelet. Next, to meet low-power low-voltage requirements, we optimize the state-space description of the filter with respect to dynamic range, sensitivity and sparsity. The filter design that follows is based on an orthonormal ladder structure and employs log-domain integrators as main building blocks. Measurements demonstrate that it approximates the required wavelet base (i.e. Morlet) in an excellent way. The tenth-order log-domain filter operates from a 1.5-V supply voltage and a total bias current of 4.3μA.

1. Introduction

The Wavelet Transform (WT) is a merited technique for analysis of non-stationary signals like cardiac signals. Being a multiscale analysis technique, it offers the possibility of selective noise filtering and reliable parameter estimation. Often WT systems employ the discrete wavelet transform, implemented in a digital signal processor. However, in ultra low-power applications such as biomedical implantable devices, it is not suitable to implement the WT by means of digital circuitry due to the high power consumption associated with the required A/D converter. Low-power analog realization of the wavelet transform enables its application in vivo, e.g. pacemakers, where the wavelet transform provides a means to extremely reliable cardiac signal detection.

2. Low-power analog wavelet filter design

The design of an analog wavelet filter, i.e., a filter that performs a WT, can be summarized by the steps shown in the procedure depicted in Fig.1. Although any function that has finite energy, is square integrable and satisfies the wavelet admissibility condition can be a wavelet [1], the discussion in this paper shall deal with the design of a Morlet wavelet filter. The Morlet wavelet base under consideration is obtained from a Gaussian envelope multiplied by a cosine function [1], and is described by $\psi(t) = \cos(5\sqrt{2}(t-3))e^{-(t-3)^2}$. In order to control the frequency range of the wavelet system and the respective

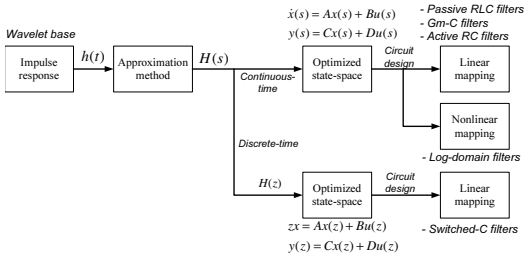

Figure 1: Analog wavelet filter design procedure.

scales, one can add a time constant term τ, resulting in

$$f(t) = \cos(\frac{5\sqrt{2}}{\tau}(t - 3\cdot\tau))e^{-(\frac{t-3\cdot\tau}{\tau})^2}. \qquad (1)$$

Its corresponding Fourier transform is given by

$$F(\omega) = \frac{\sqrt{\pi}}{2}(e^{-\frac{1}{4}(\frac{\omega-5\sqrt{2}\cdot\tau^{-1}}{\tau^{-1}})^2} + e^{-\frac{1}{4}(\frac{\omega+5\sqrt{2}\cdot\tau^{-1}}{\tau^{-1}})^2}). \quad (2)$$

The time and frequency response of the Morlet wavelet are given in Fig.2. Note that by changing τ the Q-factor of the filter remains constant and in this case is equal to 2.55.

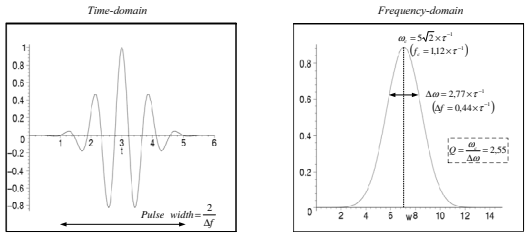

Figure 2: Ideal Morlet function. Time and frequency response .

A wavelet filter implementation is based on a bandpass filter design which presents an impulse response that equals a wavelet. The starting point of analog filter design is the definition of the respective transfer function (or differential equation). However, a linear differential equation having a predefined desired impulse response does not always exist. Thus, one is obliged to use a suitable approximation method. There are several mathematical techniques that are frequently used to achieve the best approximation possible. Nonetheless, one of the most important aspects for analog filter synthesis is that the approximating function

must lead to a physically realizable network which is dynamically stable [2].
As there are many possible state-space descriptions for a circuit that implements a certain transfer function, the designer has to find a circuit that fits his specific requirements. For low-power low-voltage applications, we optimize the state-space description of the filter for dynamic range, sensitivity and sparsity requirements [3].
The final step will be the design of the integrator, which will be the main building block of the wavelet filter. For continuous-time filters, there are basically two possible integrator types, being linear or nonlinear (e.g., log-domain). The main advantage of log-domain filters with respect to other low-power techniques is the ability to handle a large dynamic range in a low-voltage environment. Moreover, only transistors and capacitors are required to realize these functions.

2.1 Analog Wavelet bases - the need for approximation

The proposed procedure that generates a transfer function of a wavelet base (in this case a Morlet function) is based on the Padé approximation in the Laplace domain of the impulse response of the filter [2]. The Padé approximation is given by

$$F(s) = \frac{P(s)}{Q(s)} = \frac{p_0 + p_1 s + \ldots + p_m s^m}{q_0 + q_1 s + \ldots + q_n s^n} \qquad (3)$$

where $F(s)$ is the Taylor series truncated around some point, e.g. $s = 0$ and $q_n = 1$ for normalization. If the approximating rational function has a numerator of order m and a denominator of order n, the original function can be approximated up to order $m+n+1$. The computation of the coefficients of $P(s)$ and $Q(s)$ has been described in [2]. We apply a [8/10] Padé approximation, i.e., m=8 and n=10, which yields an approximation of order k=19 of the Taylor series expansion. As the main advantage of the Padé method is its computational simplicity and its general applicability, it can easily be applied to other wavelet bases as well. The resulting transfer function of the Morlet wavelet filter is $H(s) = (0.9s^8 - 13s^7 + 177s^6 - 618s^5 + 345s^4 + 7 \cdot 10^4 s^3 - 4 \cdot 10^5 s^2 + 2 \cdot 10^6 s - 3 \cdot 10^6)/(s^{10} + 13s^9 + 336s^8 + 3 \cdot 10^3 s^7 + 4 \cdot 10^4 s^6 + 2 \cdot 10^5 s^5 + 2 \cdot 10^6 s^4 + 8 \cdot 10^6 s^3 + 4 \cdot 10^7 s^2 + 9 \cdot 10^7 s + 3 \cdot 10^8)$

2.2 State-space optimization

Departing from the transfer function derived in Section 2.1, one can generate a state space description of the filter, which is optimized with respect to the Dynamic Range. In [3] a method to optimize the state space description of a dynamical system is presented, based on the observability and controllability gramians. The resulting system has, under certain conditions, the maximum dynamic range which is achievable, given the total amount of capacitance. The controllability and observability gramians are derived from the state space description. The definition of the controllability gramian is related to the system matrices A and B

$$K = \int_0^\infty e^{At} B B^T e^{A^T t} dt \qquad (4)$$

and the observability gramian is related to the system matrices A and C

$$W = \int_0^\infty e^{A^T t} C^T C e^{At} dt. \qquad (5)$$

where A, B and C are the state, input, and output matrices of the state-space description, respectively. As the dynamic range of a circuit is defined as the ratio between the maximum and the minimum signal level that it can process, optimization of the dynamic range is equivalent to the simultaneous maximization of the (distortion-less) output swing (resulting from a similarity transform of the controllability gramian) and the minimization of the overall noise contribution (by a similarity transform of the observability gramian).
Finally, profiting from the well-known fact that the relative noise contribution of an integrator decreases when the capacitance and bias current increase, we match an optimal capacitance distribution to the noise contributions of each individual integrator (noise scaling), resulting in [3]

$$C_i = \frac{\sqrt{\alpha_i w_{ii} k_{ii}}}{\sum_j \sqrt{\alpha_j w_{jj} k_{jj}}} \qquad (6)$$

where k_{ii} and w_{ii} are the main diagonal elements of K and W, respectively, $\alpha_i = \sum_j |A_{ij}|$ is the absolute sum of the elements on the i-th row of A, and C_i is the capacitance in integrator i.

2.2.1 Sparsity

The drawback of a dynamic-range optimal system is that its state-space matrices are generally fully dense, i.e., all the entries of the A, B, C matrices are filled with nonzero elements. These coefficients will have to be mapped onto circuit components, and will result in a complex circuit with a large number of interconnections. For high-order filters it is therefore necessary to investigate how a realization of the desired transfer function having sparser state-space matrices would compare to the one having maximal dynamic range. For a less complex circuit, one possibility is the Orthonormal Ladder structure [4], which is significantly sparser than the fully dense A matrix of the dynamic-range optimal system. The advantage of using this structure is its low sensitivity to coefficient mismatch. After capacitance scaling, compared to the dynamic-range optimal case, the Dynamic Range of our Morlet filter has decreased by only 1.83dB. The normalized capacitance distribution is given by $(C_1, ..., C_{10}) = C'(0.142, 0.162, 0.110, 0.117, 0.086, 0.091, 0.073, 0.080, 0.073, 0.061)$, where C' represents the unit-less value of the total capacitance when expressed in F.

2.3 Low-power log-domain integrator

Log-domain filters fall into the category known as externally linear, internally nonlinear (ELIN) systems, characterized by having a linear relation between input and output signals, while internally the signals may be nonlinearly related to the input and output. Log-domain integrators are inherently companding, i.e., the circuit's internal voltages are compressed functions of the external input and output currents. A simple bipolar multiple-input low-power log-domain integrator [5] will be used as the basic building

block for the implementation of the state space equation of a wavelet filter described in the previous section. This log-domain integrator is shown in Fig.3 [5].

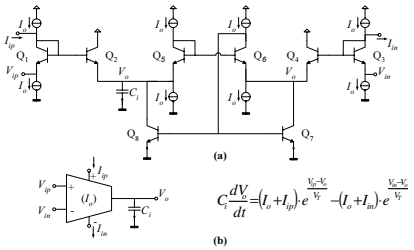

Figure 3: (a) The multiple-input low power log-domain integrator, and (b) its symbol [5].

3. Circuit design

By applying a simple mapping to the linear state-space equations, we can obtain the corresponding log-domain circuit realization which employs the log-domain integrator cell. Note that the implemented filter is a tenth order filter. The block diagram of the log-domain implementation is illustrated in Fig.4, using the universal log-domain cell symbol described in [5]. Note that each column of the filter structure corresponds to a row in the state-space formulation. The parameter A_{ij} is implemented by the corresponding log-domain integrator with bias current $I_{A_{ij}}$, defined by

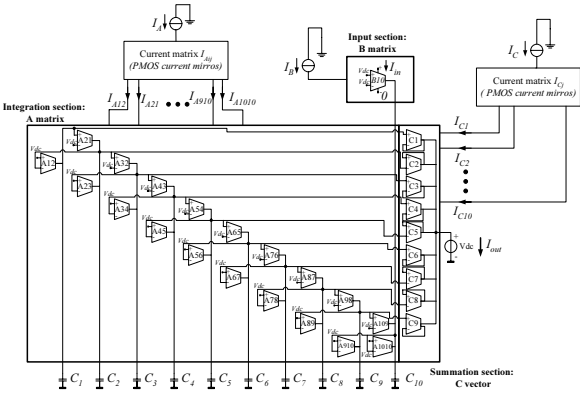

Figure 4: Complete State-space filter structure.

$$I_{A_{ij}} = A_{ij} \cdot \frac{2\pi\tau^{-1}}{2Q} C_i V_T \tag{7}$$

where τ^{-1} and Q are, the inverse of the time constant and the quality factor mentioned in Section 2., respectively, and C_i represents the i-th capacitance of the filter. The input section, as governed by the state-space vector B, can be defined as the input LOG operator and is realized by the first row from the top of Fig.4. The current I_{B_i} is related to the parameter B_i by

$$I_{B_i} = B_i \cdot \frac{2\pi\tau^{-1}}{2Q} C_i V_T \tag{8}$$

In the orthonormal case, only one non-zero parameter of the B vector is present (B_{10}). Consequently, $I_{B_i} = I_B$. Finally, in order to restore the overall system linearity one should realize the weighted summation state with the corresponding EXP operators. The bias current vector I_{C_j}, which is controlled by the vector C, is defined as

$$I_{C_j} = C_j \cdot I_B \tag{9}$$

The normalizing current I_A in Fig.4, which will control the overall time constant of the filter, is implemented by

$$I_A = \frac{I_{A_{ij}}}{\frac{W_{Aij}}{L_{Aij}}} \tag{10}$$

with $\frac{W_{Aij}}{L_{Aij}} = \frac{I_{A_{ij}(1nA)}}{1nA}$, where $\frac{W_{Aij}}{L_{Aij}}$ are the aspect ratios of the PMOS current mirrors and were defined for I_A equals to 1nA. The current I_C is obtained in a similar way.

4. Measurement results

To validate the circuit principle, we have implemented the log-domain state-space wavelet filter in IBM's $0.18\mu m$ BiCMOS IC process. A microphotograph of the circuit is shown in Fig.5.

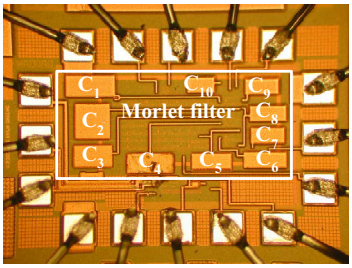

Figure 5: Chip microphotograph. The die area is $0.89mm^2$ ($0.78mm \times 1.14mm$) and the filter active area is $0.28mm^2$ ($0.35mm \times 0.79mm$).

The measurement setup is presented in Fig.6. As log-domain filters process signals in the current domain, accurate current measurements require linear transconductance and transimpedance stages at the input and at the output, respectively. These are implemented by a large resistor at the input and by a Keithley 428 nanoamp transimpedance amplifier at the output. However the transimpedance amplifier has a cutoff frequency up to 175kHz, depending on the gain factor. To be able to measure beyond 100 kHz, a transimpedance stage implemented by a low noise op amp (LF 356) and a $1k\Omega$ shunt feedback resistor is used. The cutoff frequency of this stage is 10MHz. The circuit has

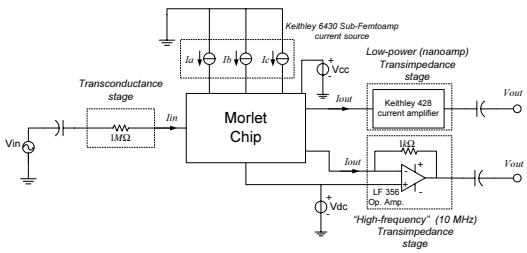

Figure 6: Measurement setup.

been designed to operate from a 1.5V supply. Fig.7 shows the measured impulse response of the wavelet filter and

the respective frequency response for $I_A = I_C = 4.3$nA and $I_B = 8.5$nA, which corresponds to $\tau^{-1} = 22 \cdot 10^3$. The transient response of the Morlet wavelet filter can be compared with the simulated filter response to confirm the performance of the log-domain filter.

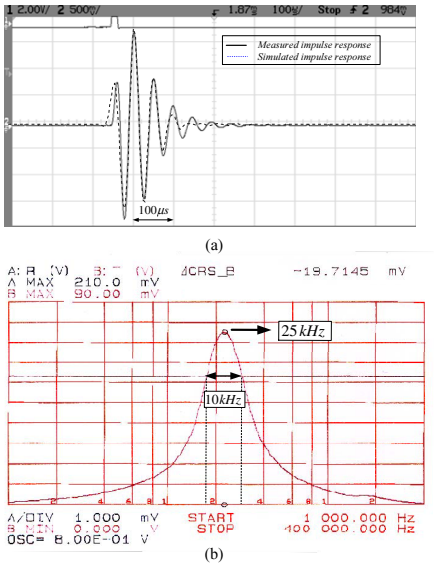

Figure 7: Measurement results (a) Measured and simulated impulse response (b) Measured frequency response.

The total filter's current consumption is 4.5μA with a $100pF$ total capacitance. The rms output current noise is 87pA, resulting in a DR at the 1-dB compression point of approximately 30dB. In addition, in order to verify the performance of the whole wavelet system, one needs to be able to scale and shift the wavelet base function. By changing the values of the bias currents accordingly, one can obtain a dyadic scale system, as illustrated in Fig.8. The current I_A has been scaled from 2nA to 8nA, resulting in a 3-scales wavelet system.

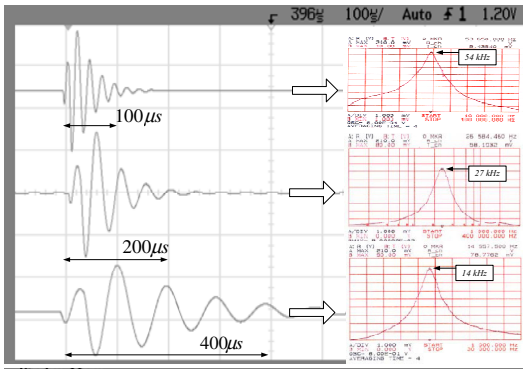

Figure 8: Measured Impulse and frequency response for 3 scales.

Finally, in order to show that the same procedure can be applied for medium frequency applications, we tuned the frequency response of the filter by varying the bias current over about three decades with center frequencies ranging from 14kHz to 8.1MHz, while preserving the impulse response waveform. Again, one can obtain the wavelet scales around this frequency (i.e. 8.1 MHz) by scaling the current, accordingly. The performance of the filter is summarized in Table I.

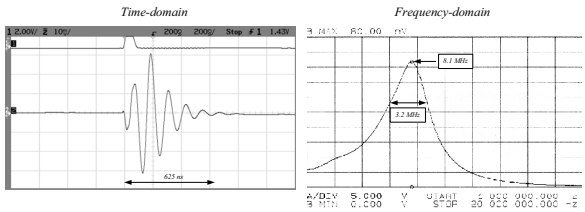

Figure 9: Time and frequency response of the Morlet filter varying the bias current I_a to $1.4\mu A$ for medium frequency operation.

Technology	0.18μm BiCMOS	
Die area	0.89mm^2	
Active area	0.28mm^2	
Bias current	$I_o = 4.3$nA	$I_o = 1.4\mu$A
Total capacitance	100pF	100pF
Supply voltage	1.5V	1.6V
Center frequency (f_c)	25kHz	8.1MHz
Power dissipation	6.75 μW	2.3mW
Dynamic Range (1-dB)	30 dB	30 dB
Noise current (rms)	87pA	64nA
Supply voltage range	1.2V - 1.8V	1.5V - 2.1V

Table 1: Performance per scale for two different operating frequencies.

5. Conclusions

A novel procedure to implement wavelet bases using analog circuitry was presented. Measurements demonstrated an excellent approximation of the Morlet wavelet base. The filter was optimized with respect to dynamic range. Moreover, sensitivity and sparsity were also taken into account in the design of the filter. Hence, the filter was able to meet the requirements imposed by a low-power environment. The circuit operates from a 1.5-V supply and a total bias current of 4.5μA. From the results obtained, we deduced that this procedure could very well be used to approximate other wavelet bases as well and to implement them on chip in an analog fashion using little power.

6. Acknowledgments

The authors would like to thank John Long, D. Harame and IBM Microelectronics for fabrication access.

References:

[1] I. Daubechies, *Ten Lectures on Wavelets*, SIAM, Philadelphia, 1992.

[2] S. A. P. Haddad, Sumit Bagga, and W. A. Serdijn, "Log-domain wavelet bases," *in Proc. ISCAS'04*, vol. 1, 2004.

[3] D. P. W. M. Rocha, *Optimal Design of Analogue Low-power Systems, A strongly directional hearing-aid adapter*, Phd thesis, TUDelft, April 2003.

[4] D. A. Johns, W. M. Snelgrove, and A. S. Sedra, "Orthonormal ladder filters," *IEEE Trans. Circuits Systs.*, vol. 36, no. 3, march 1989.

[5] G. W. Roberts and V. W. Leung, *Design and Analysis of Integrator-Based Log-Domain Filter Circuits*, Kluwer Academic Publishers, The Netherlands, 2000.